INTERFACE FOCUS

rsfs.royalsocietypublishing.org

Research

Cite this article: Berardo A, Pantano MF, Pugno NM. 2016 Slip knots and unfastening topologies enhance toughness without reducing strength of silk fibroin fibres. *Interface Focus* **6**: 20150060.
http://dx.doi.org/10.1098/rsfs.2015.0060

One contribution of 19 to a theme issue 'Integrated multiscale biomaterials experiment and modelling: towards function and pathology'.

Subject Areas:
biomaterials, nanotechnology, biomechanics

Keywords:
knots, biomaterials, toughness, fibres

Author for correspondence:
Nicola M. Pugno
e-mail: nicola.pugno@unitn.it

Slip knots and unfastening topologies enhance toughness without reducing strength of silk fibroin fibres

Alice Berardo[1], Maria F. Pantano[1] and Nicola M. Pugno[1,2,3]

[1]Laboratory of Bio-inspired and Graphene Nanomechanics, Department of Civil, Environmental and Mechanical Engineering, University of Trento, Via Mesiano 77, 38123 Trento, Italy
[2]Center for Materials and Microsystems, Fondazione Bruno Kessler, Via Sommarive 18, 38123 Povo, TN, Italy
[3]School of Engineering and Materials Science, Queen Mary University of London, Mile End Road, London E1 4NS, UK

MFP, 0000-0001-5415-920X; NMP, 0000-0003-2136-2396

The combination of high strength and high toughness is a desirable feature that structural materials should display. However, while in the past, engineers had to compromise on either strength or toughness depending on the requested application, nowadays, new toughening strategies are available to provide strong materials with high toughness. In this paper, we focus on one of such strategy, which requires no chemical treatment, but the implementation of slip knots with optimized shape and size in the involved material, which is silkworm silk in this case. In particular, a variety of slip knot topologies with different unfastening mechanisms are investigated, including even complex knots usually used in the textile industry, and their efficiency in enhancing toughness of silk fibres is discussed.

1. Introduction

The availability of materials with both high strength and high toughness is greatly desirable in structural applications, although in the past engineers had to compromise and chose one property or the other depending on the application. In fact, strong materials traditionally displayed poor deformation capability and thus low specific energy dissipation potential [1]. However, taking inspiration from nature recent developments in materials science have provided new techniques, that have already overcome the conflict between strength and toughness, such as nacre and bones, with complex structures cooperating at different length scales [2–4]. This concept has been transferred to engineering materials, introducing, for example, weak interfaces with intricate architectures [5] or dispersing fibres in a brittle matrix to form a bridge complementing crack opening and fracture [6].

While all of these solutions require some chemical treatment of the material of interest, in this paper, we considered a different toughening strategy that operates at a micro length scale and enables a significant increase in toughness of as-produced fibres. This follows an idea recently proposed by one of the authors [7] and requires the introduction of a sliding frictional element within the fibre, e.g. a knot. In fact, when the opposite ends of a knotted fibre are pulled apart, a hidden length is revealed through a sliding mechanism that dissipates a huge amount of energy. Basically, this mechanism reproduces the breakage of weak bonds (i.e. sacrificial bonds) in highly coiled macromolecules, which allow the molecular backbone to be further stretched which increases toughness [8].

The fibres considered in this study are of natural origin, as they are extracted from silkworm silk cocoons. In fact, because of its unique combination of biocompatibility, and physical and mechanical properties [9,10], silkworm silk is attracting increasing interest in a variety of biomedical applications, including tissue engineering scaffolds [11–12], drug delivery [13], sensors [14], as well as composites [15]. Such interest motivates the need to further improve the properties of silk, such as its energy dissipation capability (i.e. toughness) [16].

THE ROYAL SOCIETY PUBLISHING

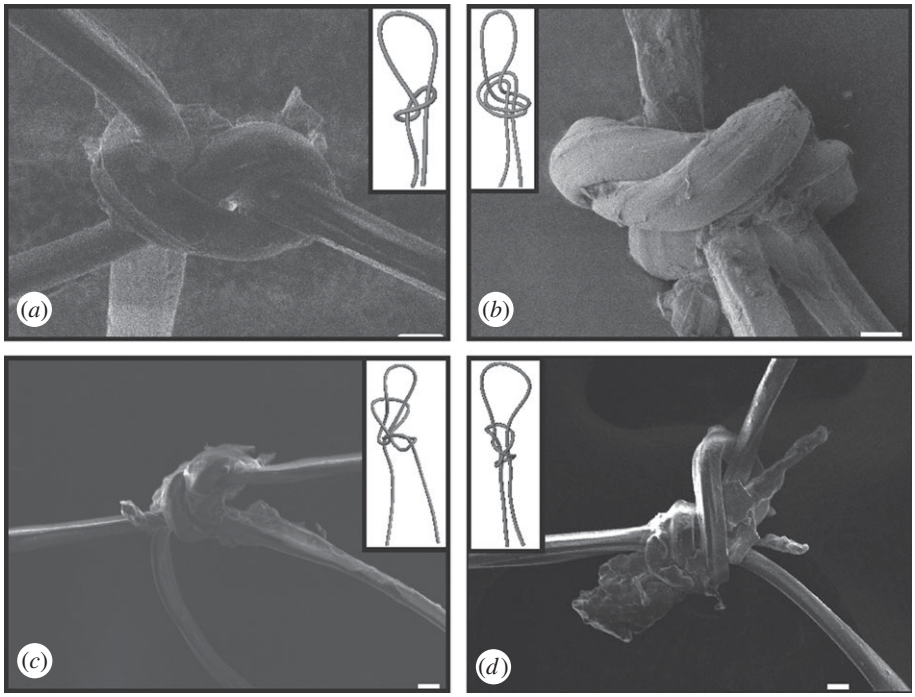

Figure 1. Gallery of knots implemented in single silk fibres. (*a*) SEM picture of the *noose* with a schematic on top. (*b*) SEM picture of the *overhand loop* with a schematic on top. (*c*) SEM picture of the *chain knot* with two chains and a schematic on top. (*d*) SEM picture of the *X-knot* with a schematic on top. Scale bar, 10 µm.

In this paper, the toughness of single silk fibres was increased through the introduction of knots with optimized shape and size. In fact, different kinds of knots can be encountered in everyday life as well as in a variety of fields with studies reporting the application of knots in mathematics [17], polymer science [18,19], colloids [20,21], fluids [22], chemistry [23,24] and biology [25,26]. However, in this paper, we investigated those topologies which enable maximization of toughness without compromising fibre strength. For this reason, as in our earlier work [27], our attention was focused on slip or running knots, which can be unfastened without inducing stress concentration and premature failure in the fibre. In the following, four topologies are considered, involving different unfastening mechanisms and design complexities (some of which are well known in textile industry), with the aim of providing new and feasible tools for optimizing systems where energy dissipation is much sort after.

2. Methods

2.1. Preparation of samples with different slip knot topologies

In the following sections, we report experiments carried out on single fibres extracted from *Bombyx mori* silkworm silk cocoons. In particular, before fibre extraction, as-produced cocoons underwent a standard degumming process [28], consisting of boiling twice with 1.1 and 0.4 g l^{-1} Na_2CO_3 (anhydrous, minimum 99%, from Sigma Aldrich) water solution for 1 h each time, washing against distilled water and air-drying. In this way, it was possible to obtain silk fibroin fibres released from their natural binding layer (i.e. sericin), which has no load bearing capacity [29].

Then, single fibroin fibres were manipulated by tweezers in order to design knots with the appropriate topology. The knots implemented in our experiments were chosen in order to guarantee that the fibre was highly stressed within a sufficiently large strain interval when its opposite ends are pulled apart (as during a tensile test), but without introducing stress concentration, which could lead to premature failure. Under these conditions, in fact, the introduction of a knot is able to modify the stress–strain curve of the fibres, introducing an artificial plastic-like plateau with a significant increase in toughness [7].

In order for the knot not to affect the fibre strength, it is necessary that the knot can be completely released as the fibre ends are pulled apart. Thus, only slip knots were herein considered. In our earlier work [27], we implemented two different slip knot topologies in single silk fibres, which are known as *noose* and *overhand loop* [30] (figure 1*a*,*b*). While the *noose* requires the fibre to be turned once around on itself, the *overhand loop* requires the fibre to be first folded and then turned around on itself, thus involving a different unfastening mechanism. In fact, in the first case, the knot tends to untie as the fibre ends are pulled apart. Thus, at the beginning, this can be very tight causing the fibre to be highly stressed during the whole tensile test and its toughness to be significantly increased. On the contrary, in the *overhand loop*, the knot tends to further tie, requiring a very loose initial configuration in order to be released completely, resulting in considerable less toughness in the material. As a consequence, in this work, we investigated and optimized other slip knot topologies that are strictly related to the *noose* in order to further improve our previous results.

The first topology we considered is an open version of the *monkey chain lanyard knot* [30], which is well known in the textile industry, as this reproduces a chain stitch of crochet (figure 1*c*): after a noose is tightened, one thread of the fibre is folded and forced to cross the loop, which ends in a chain of a chain stitch. In some samples, such steps were repeated in order to build chain stitch with four and six chains, respectively. In the following, for the sake of brevity, this knot topology will be referred to as simply a *chain knot*.

The second topology (figure 1*d*), which has no common name, requires the implementation of a noose [30]; then, its loop is turned inside the knot, obtaining an X-shaped knot, which is referred to as the *X-knot* topology in the following.

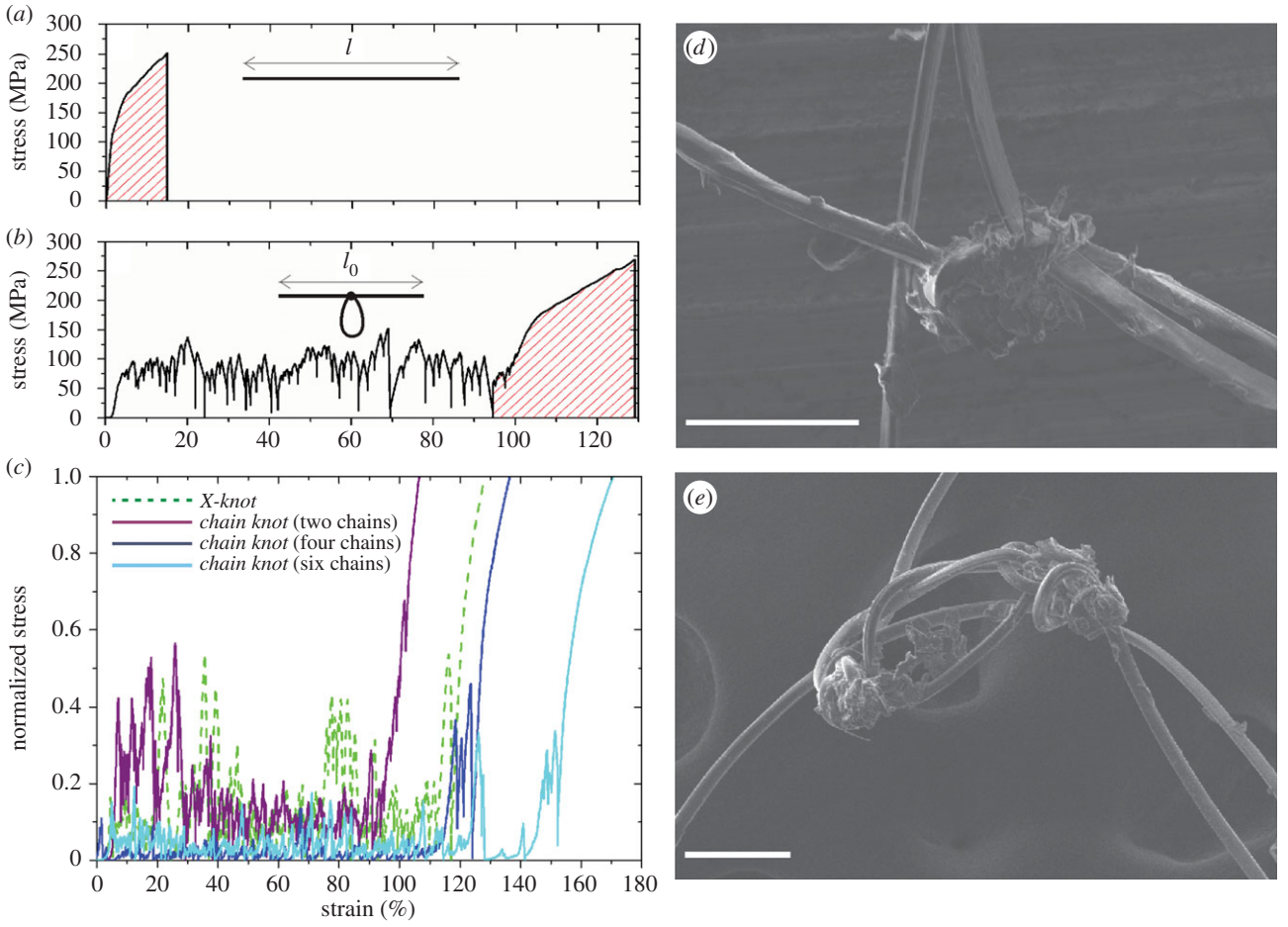

Figure 2. (*a*) Stress–strain curve of an unknotted natural fibre with length *l*. (*b*) Stress–strain curve of a knotted natural fibre with length *l* and distance between its opposite ends l_0, which was extracted from a cocoon region adjacent to the unknotted fibre (*a*). The presence of the knot modifies the shape of the stress–strain curve (*a*), introducing a plastic-like plateau and leaving a final region (highlighted) almost corresponding to the stress–strain curve of the same fibre with unknotted configuration. The strain interval within this final region appears larger than in (*a*) because it is computed with respect to l_0 instead of *l*. (*c*) Comparison between the stress–strain curves derived from samples with an *X-knot* and a *chain knot* with either two, four or six chains, respectively. Here, stress values are normalized with respect to the fracture stress of each fibre. (*d*) SEM image of a fibre with a *chain knot* with four chains visibly damaged by preparation, which caused superficial exfoliation. (*e*) SEM image of a fibre with a *chain knot* with six chains not uniformly tightened during preparation. Scale bar, 100 µm. (Online version in colour.)

All the samples were obtained from a fibre with initial length (l) equal to 20 mm, mounted on a paper frame in order for the fibre ends to be 10 mm apart (l_0) and with a length of about 10 mm involved in the loop (l_p) (figure 2*a*,*b*).

2.2. Estimation of toughness increase due to knots

The energy per unit mass (i.e. toughness modulus, T_u) dissipated by an unknotted fibre during a tensile test is related to the area under its stress–strain curve (figure 2*a*) as

$$T_u = \frac{1}{m}\int_0^{x_f} F\,dx = \frac{Al}{m}\int_0^{\varepsilon_f} \sigma\,d\varepsilon = \frac{1}{\rho}\int_0^{\varepsilon_f} \sigma\,d\varepsilon, \qquad (2.1)$$

where m is the fibre mass, x_f is the displacement at fracture, F is the applied load, A is the fibre cross-sectional area, l is the fibre initial length, ρ is the volumetric density, $\varepsilon_f = (l_f - l)/l = x_f/l$ is the fracture strain, l_f is the fibre final length and $\int_0^{\varepsilon_f} \sigma d\varepsilon$ is the area under the stress–strain curve.

If a knot is introduced in a fibre (figure 2*b*), expression (2.1) has to be modified in order to take into account the length of fibre involved in both the knot (negligible) and the loop, with its toughness modulus, T_k, which can be computed as

$$T_k = \frac{1}{m}\int_0^{x_f^*} F dx = \frac{Al_0}{m}\int_0^{\varepsilon_f^*} \sigma d\varepsilon = \frac{1-k_1}{\rho}\int_0^{\varepsilon_f^*} \sigma d\varepsilon, \qquad (2.2)$$

where $x_f^* = l - l_0 + x_f$, l_0 is the initial length equal to the distance between the ends of the fibre, $\varepsilon_f^* = x_f^*/l_0$, $k_1 = (l - l_0)/l$ accounting for the difference between l_0 and l and $\int_0^{\varepsilon_f^*} \sigma d\varepsilon$ is the area under the stress–strain curve of the knotted fibre [7].

When the opposite ends of a knotted fibre are pulled apart, the knot causes alternating cycles of loading (the knot is tightened and the fibre is stressed) and unloading (the knot unties, a length of fibre is released from the loop, causing stress relaxation) until the knot loosens completely (figure 2*b*). In all our tests, the final part of the stress–strain curve of knotted fibres reproduced the stress–strain curve of the corresponding unknotted fibres, showing, in fact, a stress at breakage comparable with the strength of reference samples (without any knots and extracted from a cocoon region adjacent to the knotted fibre) tested separately (figure 2*a*,*b*). Moreover, because it is well known that the mechanical properties of silk show significant variability [31], it is preferable to compare the toughness of a knotted fibre with the toughness of the same fibre in unknotted configuration. For this reason, we considered the final part of the stress–strain curve of a knotted fibre as the curve of its reference unknotted fibre. Then, the ratio between the toughness of the knotted fibre, T_k, and the toughness of the corresponding unknotted fibre, T_u', can be obtained with the following expression

$$\frac{T_k}{T_u'} = \frac{Al_0/m\int_0^{\varepsilon_f^*} \sigma\,d\varepsilon}{Al_0/m\int_{\varepsilon^*}^{\varepsilon_f^*} \sigma\,d\varepsilon} = \frac{\int_0^{\varepsilon_f^*} \sigma\,d\varepsilon}{\int_{\varepsilon^*}^{\varepsilon_f^*} \sigma\,d\varepsilon}, \qquad (2.3)$$

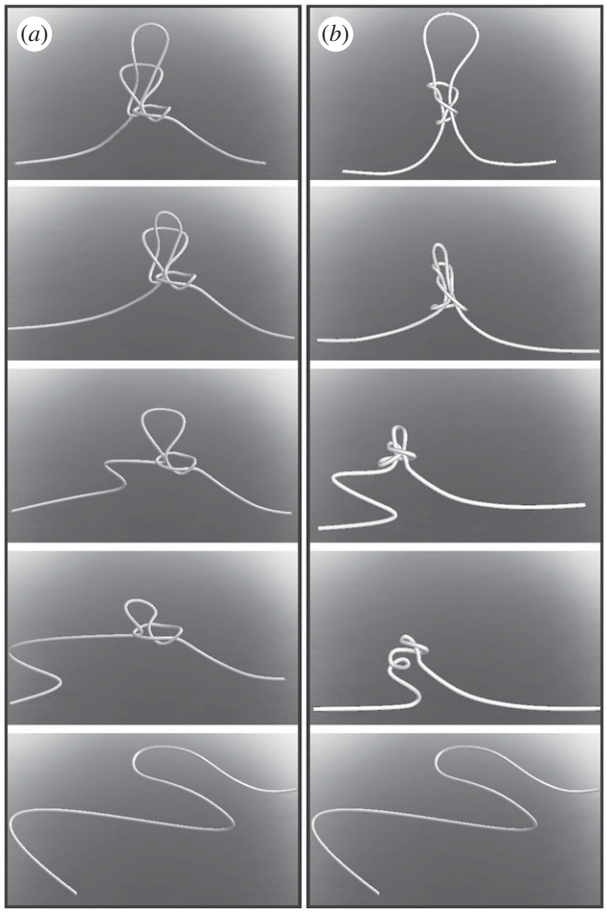

Figure 3. Untightening mechanism of the (*a*) *chain knot* (in this schematic with two chains) and (*b*) *X-knot*. (*a*) When the fibre opposite ends are pulled apart, the loop is sucked into its closest chain until this is completely released, thus forcing the knot to collapse into a simple noose. If the fibre ends are pulled further apart, then the noose loosens until the knot is completely untightened. (*b*) In an *X-knot*, the fibre appears to be turned twice at the bottom of its loop. When its opposite ends are pulled apart, the turn closer to the loop tends to tie, causing friction against fibre sliding, whereas the other one loosens. In this way, the knot is always able to completely unfasten but a significant amount of energy can be dissipated. (Online version in colour.)

where $\int_{\varepsilon^*}^{\varepsilon_f} \sigma \mathrm{d}\varepsilon$ is the area under the final part of the stress–strain curve, where the knot is completely released.

However, in case it is not possible to consider the same fibre for comparison, because the final part of the stress–strain curve does not clearly show the behaviour of the fibre in unknotted configuration, we can estimate the toughness increase referring to the toughness modulus of an unknotted fibre extracted from a cocoon region adjacent to that of the knotted fibre in order to limit variations in physical and mechanical properties. In this way, the area under the stress–strain curve of the knotted fibre has to be scaled by the factor $(1 - k_1)$

$$\frac{T_k}{T_u} = \frac{(1-k_1)/\rho \int_0^{\varepsilon_f^*} \sigma \mathrm{d}\varepsilon}{1/\rho \int_0^{\varepsilon_f} \sigma \mathrm{d}\varepsilon} = \frac{(1-k_1) \int_0^{\varepsilon_f^*} \sigma \mathrm{d}\varepsilon}{\int_0^{\varepsilon_f} \sigma \mathrm{d}\varepsilon}. \qquad (2.4)$$

3. Results

To evaluate the toughness enhancement owing to knot introduction, we performed tensile tests on more than 50 samples knotted in either of the topologies described in the previous sections. Tests were carried out at room temperature at a strain rate of $0.002\ \mathrm{s}^{-1}$ by a nanotensile testing machine (Agilent T150 UTM). Following a common approach reported in the literature [29], stress was computed considering each fibre as having a circular cross section, which was evaluated using an optical microscope and scanning electron microscope (SEM). The average diameter of the fibres was 11.5 ± 1.5 µm. All knotted fibres broke at a stress level of about 420 ± 130 MPa, which matches the typical strength of pristine silk fibres.

Figure 2*c* reports four stress–strain curves, one for each knot topology tested. In all the cases, with respect to the stress–strain curve of a sample with no knots (figure 2*a*), there is a series of loading and unloading events caused by the fibre sliding into its loop through the knot and related stick–slips, as explained in §2.2. Furthermore, it is interesting to observe that at the end of the test, before the knot loosens completely and the curve collapses into the stress–strain curve of an unknotted fibre, there are some pronounced stress peaks, which correspond to the number of times the fibre was turned around on itself during preparation. In fact, the number of final stress peaks, which is the main factor responsible for toughness increase, is more visible in the case of a chain knot with four and six chains.

As evolutions of the *noose*, all knot topologies could be firmly tightened and then completely unfastened during the test with quite high-energy dissipation (table 1), depending on the stress plateau value introduced in the corresponding stress–strain curve (figure 2*c*). In particular, samples with a chain knot with two chains showed a stress–strain curve with a well-defined plastic-like plateau between one-eighth and a quarter of the fracture strength (figure 2*c*), providing a toughness increase of about 300%, which is comparable to the result obtained with the *noose* [27]. When the number of chains is

Table 1. Comparison (*) between the toughness increases and strength decreases provided by different knot topologies with respect to unknotted single silk fibres (average strength of 514 ± 103 MPa and average toughness modulus: 32 ± 14 J/g computed considering a density of 1.4 g/cm^3 [32]).

knot topology	number of test	toughness increase (%)	strength decrease (%)
noose	14	284 ± 43	32 ± 29
overhand loop	20	118 ± 19	21 ± 37
X-knot	8	450 ± 107	18 ± 27
chain knot with 2 chains	11	310 ± 11	7 ± 35
chain knot with 4 chains	6	150 ± 11	19 ± 27
chain knot with 6 chains	5	142 ± 18	11 ± 30

(*) Because of variability in the knot tightening procedure, the knot size shows some difference from sample to sample. Thus, when we computed the toughness enhancement provided by each knot topology, we considered an average over three results representative of their optimized behaviour.

increased, there is no evident trend in toughness enhancement (table 1). In fact, although some samples with a chain knot with four chains provided significant toughness enhancement of almost 400%, the average value is much lower, being about 150%, which is comparable to the average result provided by chain knots with six chains. However, such values are still greater than that recorded for the *overhand loop* (table 1).

On the contrary, *X-knot* topology, providing a higher plateau in the stress–strain curve of the samples, with average values of about one-fifth of the fracture stress (figure 2*c*) resulting in a toughness enhancement of up to 450% on average (table 1).

4. Discussion

In order to understand the differences in toughness enhancement provided by the investigated knot topologies (table 1), it is necessary to consider the preparation procedure and unfastening mechanism of the knots (figure 3). As we reported in [27], in this case, the lowest toughness enhancement was also provided by the *overhand loop*. In fact, this is the only topology where the knot tends to further tie as the opposite ends of its hosting fibre are pulled apart. As a consequence, this is able to completely unfasten only when its initial configuration is loose, thus causing low friction against fibre sliding and a consequent limited increase in toughness. On the contrary, the *noose* can be very tight in its initial configuration, providing a high and wide plateau in the fibre stress–strain curve, which causes the toughness enhancement to be much higher (table 1).

Although the other knots considered in this work, the *chain knot* and *X-knot*, both evolve from the *noose*, they provided different results, which depend on the different sliding mechanisms experienced by the fibre before the knot completely unfastens (figure 3). In this context, the *chain knot* behaves more similar to the *noose*, because the chain, which is closer to the loop, tends to open as the fibre ends are pulled apart, thus the fibre can slide easily within the loop and the knot tends to further untie (figure 3). On the contrary, part of the *X-knot* tends to tie when the fibre is pulled (figure 3). In this case, the fibre appears to be turned twice, but while one turn (which is the closest to the loop) tends to tie, the second turn (on the opposite side) tends to untie as the fibre ends are pulled apart. This means that the knot can always be released, but with significant energy dissipation, causing the fibre to be much more stressed during the test and the toughness induced is more than four times greater than the reference (table 1).

We also investigated the influence of the number of chains on the friction potential of the *chain knot*. Compared with other knots, chain knots with multiple chains require increasing manipulation, which in turn induces superficial exfoliation in the knotted fibre (figure 2*d*). This could contribute to enhancing the energy dissipated by friction during unfastening, as the surface of the fibre becomes rougher, but it could also affect the fibre fracture strength, if excessive damage is introduced. From a quantitative point of view, our results show that the introduction of two chains in the chain knot provided approximately a twofold increase in toughness with respect to the average data obtained with four and six chains, which were comparable (table 1). This indicates that in the latter cases, the friction potential was not fully exploited, as it was difficult to guarantee all chains in the knot would be uniformly tightened (figure 2*e*). Nevertheless, in some cases, we achieved a much more significant increase of almost 400%, meaning that there is still room for further increases, which could be achieved through implementation of a controlled and repeatable production process, as that used in textile industry, where this knot is already commonly applied.

5. Conclusion

In this paper, we compared the effectiveness of different knot topologies to enhance the toughness of single silk fibres. The knots considered herein were characterized by different design complexity, but all had the common feature that they could be completely unfastened when the ends of the fibre were pulled apart. This condition prevented stress concentration in the fibre, which could cause premature failure of the fibre, and enabled dissipation of a significant amount of energy, depending on the knot design. Such results are very promising, because some of the tested knots are already known in the textile industry. Thus, the availability of industrial machinery able to process the knots with high quality and repeatability could easily allow them to be implemented in industrial products requiring energy dissipation capabilities.

Competing interests. We have no competing interests.

Funding. N.M.P. is supported by the European Research Council (ERC StG Ideas 2011 BIHSNAM no. 279985 on 'Bio-Inspired hierarchical super-nanomaterials', ERC PoC 2015 SILKENE no. 693670 on 'Bionic silk with graphene or other nanomaterials spun by silkworms', ERC PoC 2013-2 KNOTOUGH no. 632277 on 'Super-tough knotted fibres'), by the European Commission under the Graphene Flagship (WP10 'Nanocomposites', no. 604391) and by the Provincia Autonoma di Trento ('Graphene Nanocomposites', no. S116/2012-242637 and reg.delib. no. 2266).

Acknowledgements. The authors thank Nello Serra from 'Comunità don Milani' (Acri, CS, Italy) for kindly supplying the silk cocoons used in the experiments.

References

1. Ritchie RO. 2011 The conflicts between strength and toughness. *Nat. Mater.* **10**, 817–822. (doi:10.1038/nmat3115)
2. Bouville F, Maire E, Meille S, Van de Moortèle B, Stevenson AJ, Deville S. 2014 Strong, tough and stiff bioinspired ceramics from brittle constituents. *Nat. Mater.* **13**, 508–514. (doi:10.1038/nmat3915)
3. Munch E, Launey ME, Alsem DH, Saiz E, Tomsia AP, Ritchie RO. 2008 Tough, bio-inspired hybrid materials. *Science* **5907**, 1516–1520. (doi:10.1126/science.1164865)
4. Cranford SW, Tarakanova A, Pugno N, Buehler MJ. 2012 Nonlinear material behaviour of spider silk yields robust webs. *Nature* **482**, 72–78. (doi:10.1038/nature10739)
5. Mirkhalaf M, Khayer Dastjerdi A, Barthelat F. 2013 Overcoming the brittleness of glass through bio-inspiration and micro-architecture. *Nat. Commun.* **5**, 3166.
6. Palmeri MJ, Putz KW, Brinson LC. 2010 Sacrificial bonds in stacked-cup carbon nanofibers: biomimetic toughening mechanisms for composite systems. *ACS Nano* **4**, 4256–4264. (doi:10.1021/nn100661a)

7. Pugno NM. 2014 The "egg of Columbus" for making the world's toughest fibres. *PLoS ONE* **9**, e93079. (doi:10.1371/journal.pone.0093079)
8. Fantner GE *et al.* 2006 Sacrificial bonds and hidden length: unraveling molecular mesostructures in tough materials. *Biophys. J.* **90**, 1411–1418. (doi:10.1529/biophysj.105.069344)
9. Perez-Rigueiro J, Viney C, Llorca J, Elices MJ. 1998 Silkworm silk as an engineering material. *J. Appl. Polym. Sci.* **70**, 2439–2447. (doi:10.1002/(SICI)1097-4628(19981219)70:12<2439::AID-APP16>3.0.CO;2-J)
10. Altman HG, Diaz F, Jakuba C, Calabro T, Horan RL, Chen J, Lu H, Richmond J, Kaplan DL. 2003 Silk-based biomaterials. *Biomaterials* **24**, 401–416. (doi:10.1016/S0142-9612(02)00353-8)
11. Ude AU, Ariffin AK, Azhari CH. 2013 An experimental investigation on the response of woven natural silk fiber/epoxy sandwich composite panels under low velocity impact. *Fiber Polym.* **14**, 127–132. (doi:10.1007/s12221-013-0127-2)
12. Yodmuang S *et al.* 2015 Silk microfiber-reinforced silk hydrogel composites for functional cartilage tissue repair. *Acta Biomater.* **11**, 27–36. (doi:10.1016/j.actbio.2014.09.032)
13. Meinel AJ, Kubowb KE, Klotzsch E, Garcia-Fuentes M, Smith ML, Vogel V, Merkle HP, Meinel L. 2009 Optimization strategies for electrospun silk fibroin tissue engineering scaffolds. *Biomaterials* **30**, 3058–3067. (doi:10.1016/j.biomaterials.2009.01.054)
14. Tsioris K, Tilburey GE, Murphy AR, Domachuk P, Kaplan DL, Omenetto FG. 2010 Functionalized-silk-based active optofluidic devices. *Adv. Funct. Mater.* **20**, 1083–1089. (doi:10.1002/adfm.200902050)
15. Hardy JG, Romer LM, Scheibel TR. 2008 Polymeric materials based on silk proteins. *Polymer* **49**, 4309–4327. (doi:10.1016/j.polymer.2008.08.006)
16. Shao Z, Vollrath F. 2002 Surprising strength of silkworm silk. *Nature* **418**, 741. (doi:10.1038/418741a)
17. Anstee RP, Przytycki JH, Rolfsen D. 1989 Knot polynomials and generalized mutation. *Topol. Appl.* **32**, 237–249. (doi:10.1016/0166-8641(89) 90031-X)
18. Bayer RK. 1994 Structure transfer from a polymeric melt to the solid state—part III: influence of knots on structure and mechanical properties of semicrystalline polymers. *Colloid Polym. Sci.* **272**, 910–932. (doi:10.1007/BF00658889)
19. Saitta AM, Soper PD, Wasserman E, Klein ML. 1999 Influence of a knot on the strength of a polymer strand. *Nature* **399**, 46–48. (doi:10.1038/19935)
20. Tkalec U, Ravnik M, Copar S, Zumer S, Musevic I. 2011 Reconfigurable knots and links in chiral nematic colloids. *Science* **333**, 62. (doi:10.1126/science.1205705)
21. Sennyuk B, Liu Q, He S, Kamien RD, Kusner RB, Lubensky TC, Smalyukh I. 2013 Topological colloids. *Nature* **493**, 200–205. (doi:10.1038/nature11710)
22. Kleckner D, Irvine WTM. 2013 Creation and dynamics of knotted vortices. *Nat. Phys.* **9**, 253–258. (doi:10.1038/nphys2560)
23. Forgan RS, Sauvage JP, Stoddart JF. 2011 Chemical topology: complex molecular knots, links and entanglements. *Chem. Rev.* **111**, 5434–5464. (doi:10.1021/cr200034u)
24. Ayme JF, Beves JE, Leigh DA, McBurney RT, Rissanen K, Schultz D. 2012 A synthetic molecular pentafoil knot. *Nat. Chem.* **4**, 15–20. (doi:10.1038/nchem.1193)
25. Dean F, Stasiak A, Koller T, Cozzarelli N. 1985 Duplex DNA knots produced by *Escherichia coli* topoisomerase I. Structure and requirements for formation. *J. Biol. Chem.* **260**, 4975–4983.
26. He C, Lamour G, Xiao A, Gsponer J, Li H. 2014 Mechanically tightening a protein slipknot into a trefoil knot. *J. Am. Soc. Chem.* (doi:10.1021/ja503997h)
27. Pantano MF, Berardo A, Pugno N. 2015 Tightening slip knots in raw and degummed silk to increase toughness without losing strength. *Sci. Rep.* **5**, 18222. (doi:10.1038/srep18222)
28. Bonani W, Maniglio D, Motta A, Tan W, Migliaresi C. 2011 Biohybrid nanofiber constructs with anisotropic biomechanical properties. *J. Biomed. Mater. Res. B.* **96**, 276–286. (doi:10.1002/jbm.b.31763)
29. Perez-Rigueiro J, Viney C, Llorca J, Elices M. 2000 Mechanical properties of single-brin silkworm silk. *J. Appl. Polym. Sci.* **75**, 1270–1277. (doi:10.1002/(SICI)1097-4628(20000307)75:10<1270::AID-APP8>3.0.CO;2-C)
30. Ashley CW. 1944 *The Ashley book of knots*. New York, NY: Doubleday, Doran and Co. Inc.
31. Zhao HP, Feng XQ, Shi HJ. 2007 Variability in mechanical properties of *Bombyx mori* silk. *Mater. Sci. Eng. C* **27**, 675–683. (doi:10.1016/j.msec.2006.06.031)
32. Ashby MF. 2011 *Materials selection in mechanical design*. Burlington, MA: Butterworth-Heinemann.